Getting Closer to Reality? Peak-Shaving with Battery Systems in Commerce and Industry

Arne Groß(✉), Lars Kreilgaard, Benedikt Köpfer, and Matthias Kühnbach

Department Smart Grids, Fraunhofer Institute for Solar Energy Systems, Freiburg, Germany
arne.gross@ise.fraunhofer.de

Abstract. With decreasing prices of batteries, business cases of electric storage systems reach profitability in commercial applications. However, for commercial storage systems to become economically attractive, many studies indicate that different use cases both behind and in front of the meter must be addressed simultaneously. Shaving load peaks to reduce grid surcharges is considered in most presented setups. However, the success of weighing peak-shaving with other use cases is highly dependent on a precise load forecast.

In the literature, perfect foresight of the future load profile is assumed for most multi-use applications. In a real-life setup, forecasts have sizable uncertainty specifically for load peaks. Consequently, the performance of a storage system in a realistic setting could differ vastly.

Addressing this topic, this article presents an Energy Management System (EMS) for a battery storage combining peak-shaving with other use cases. The EMS relies on machine learning techniques tailored specifically to forecast load peaks and a heuristic control scheme using these forecasts in operation.

Furthermore, we compare the performance using our load forecast algorithm to the operation with perfect foresight.

Keywords: PV Battery Systems · Forecast of Electrical Load · Peak Shaving · Multi-Use

1 Introduction

Two main goals of the transition to a renewable energy system are the integration of volatile renewable energy sources and the electrification of emission intensive processes such as transport and heating. The integration into existing electricity grids increases the need for energy management to assure stability. To motivate end users to a favorable consumption behavior, many market measures have been implemented in recent years.

For commercial and industrial (C&I) end users, this offers various chances to reduce energy costs or to establish new revenue streams. Wüllner et al. published

P. Schossig et al. (Eds.): IRES 2022, AHE 16, pp. 193–205, 2023.
https://doi.org/10.2991/978-94-6463-156-2_14

a detailed overview over current and future business cases in the C&I sector. Additional they review the potential of battery energy storage systems (BESS) for single use cases.

These cases can be roughly divided into grid services and customer services. The participation in grid services such as frequency containment reserve (FCR) open additional revenue streams for companies, whereas customer services such as peak-shaving result in energy cost savings. In Germany, applying an "atypical grid usage" can reduce the grid fees by up to 80%. To benefit from atypical grid usage, a company has to reduce the peak load in time intervals of high grid usage predetermined by the grid operator. Due to a lack of flexibility in internal processes many companies struggle to benefit from this regulation. This results in competitive disadvantage compared to companies which are able to take advantage of the energy market rules. BESS are able to provide the necessary flexibility to financially profit from various use-cases.

With a lifespan of 10–15 years the purchase of a battery is a long-term investment which results in high investments. This is one of the main barrier for companies to refrain from a BESS installation.

In the last years falling battery prices reduced this investment and led to a strongly growing market [6]. Simultaneously, increasing energy prices enlarge the potential revenue streams. However, most use-cases, when applied as a single use-case, are financially not attractive, although this is highly dependent on the specific company. Sometimes a BESS solely used for peak-shaving, which is currently the most profitable use-case, already pays off.

In other cases, the implementation of a BESS can be profitable by stacking multiple revenue streams. For example, both references [3] and [5] demonstrate that combining peak-shaving with the provision of frequency containment reserve (FCR) and spot market trading (SMT) results in higher profitability. In general, a multi-use concept can be established by distinguishing different periods to assign them to different use cases (so called sequential multi-use). A popular case is to combine atypical grid usage with the provisioning of FCR as typically atypical grid usage leaves periods of several months without restrictions from the grid operator [2].

All multi-use concepts have in common that an intelligent operation strategy is essential to maximize the benefits of a BESS This requires not only good knowledge, but also a good forecast of the behavior of the energy system. Most published studies avoid the aspect of good forecast of the energy system by assuming a perfect forecast. For the application of operation algorithms in real energy systems, this is not a valid assumption.

In this paper we address the problem of operating a BESS under the uncertainty of load forecasting in a multi-use setting. The considered multi-use case is the combination of peak-shaving and simultaneous increase of self-consumption. In a simulation, our multi-use control algorithm using different forecasts is compared to perfect forecast case. Furthermore, we show its potential advantage compared to control algorithms addressing only a single use case.

We begin with an overview of the challenges when predicting peak loads in Sect. 2. Then in Sect. 3 the energy and BESS model is introduced. The use-cases peak-shaving and self-sufficiency are described, and the control concept is defined. The results of this approach are compared in Sect. 4. Finally, the results are discussed and planned work is presented in Sect. 5.

2 Forecasting Peaks of Electric Load

Forecasting electric load is a widely explored topic with textbooks introducing the main principles [8]. Studies reviewing the extensive scientific output in the field can be found in [1,10,12].

However, most of the studies typically consider the root mean squared error (RMSE) as the main error measure. This is very helpful in many applications as methods optimized on a low RMSE predict the expected energy of a power profile well. In contrast, the RMSE can not describe the accuracy when forecasting load peaks. Hence, most forecasts perform suboptimally in this domain.

In commercial applications, peak grid consumption is costly. Therefore, there is a strong motivation to evaluate forecasts based on the ability to forecast peaks and improve the accuracy.

In this Section we present common measurements for peak accuracy and evaluate early methods based on these indicators.

2.1 Forecast Methods

We make use of an earlier work where we have compared different forecast methods using machine learning [7]. All methods use the data of the past 90 days in order to predict the upcoming day. This data is enriched with calendric data as features to learn a mapping from these features to the power profile. Subsequently, the mapping is used once a day to generate a day-ahead forecast from the features from every point in time over the day.

Out of the methods reviewed in [7] we have selected the following to be applied.

- **Persistence (Pers)**: This approach is using the naïve assumption that the load profile is similar to the load profile exactly one week prior.
- **Multi Layer Perceptron (MLP)**: A neuronal network is used. It has two dense layers with 162 neurons each. The activation function is a rectified linear unit function, and a sigmoid function in the first and second hidden layer respectively. The learning rate, batchsize, and number of epochs are 0.0018, 128, and 500 respectively.
- **Generalized Linear Model (GLM)**: A linear dependence between the features and the load is fitted on the data. Here, we use a Gaussian link function.
- **K-Nearest-Neighbor (KNN)**: In KNN regression, similar points in the training data are identified based on a Euclidean distance in the feature space. Then, the forecast for a specific point in time is the average of the respective load values. Here, we use a number of 40 neighbors.

2.2 Metrics for Forecast Accuracy

Using the above methods we generate forecasts for the year that we evaluate using the following metrics.

The forecasts have a time resolution of $\Delta t^{\mathrm{fc}} = 15\,\mathrm{min}$. Each forecast consists of $F = 96$ values equivalent to a day-ahead forecast numbered using the index f

$$\bar{p}^{\mathrm{l}} = (\bar{p}^{\mathrm{l}}_0, \ldots, \bar{p}_f,^{\mathrm{l}} \ldots, \bar{p}^{\mathrm{l}}_{F-1}) \tag{1}$$

where we use the notation without an index to denote the full time series of the load with the superscript l. A bar above the variable indicates that the respected quantity is a forecast of the measured variable

$$p^{\mathrm{l}} = (p^{\mathrm{l}}_0, \ldots, p^{\mathrm{l}}_{F-1}). \tag{2}$$

Forecast metrics typically rely on characteristics of the complete day-ahead forecast. We therefore introduce the notation

$$\bar{p}^{\mathrm{l}}(d) \tag{3}$$

to denote the day-ahead forecast for day d out of the $D = 365$ days of a year.

A standard measure to evaluate forecasts is the root mean squared error (RMSE) that we calculate over the whole year

$$\mathrm{RMSE} = \sqrt{\sum_{d=0}^{D-1} \sum_{f=0}^{F-1} \frac{(p^{\mathrm{l}}_f(d) - \bar{p}^{\mathrm{l}}_f(d))^2}{F * D}}. \tag{4}$$

As this studies focus on forecasting the peak load of an industrial actor, the used metrics have to be adapted to this objective. Some metrics to this end are presented in [4].

The peak absolute percentage error (PAPE) expresses the difference of predicted peak power to the observed peak power. It is defined as

$$\mathrm{PAPE} = \frac{100\%}{D} \sum_{d=0}^{D-1} |\max(\bar{p}^{\mathrm{l}}(d)) - \max(p^{\mathrm{l}}(d))|. \tag{5}$$

For the battery control, the expected energy consumed above a certain limit power p^{lim} is important as it has to be covered by the battery. We describe the forecast accuracy for this quantity using the RMSE of the energy above the peak $\mathrm{RMSE}^{\mathrm{abv}}$ on each day.

To this end we define the energy above the threshold as

$$E^{\mathrm{abv}}(\bar{p}^{\mathrm{l}}(d)) = \sum_{f=0}^{F-1} \max(0, \bar{p}^{\mathrm{l}}_f(d) - p^{\mathrm{lim}}) \Delta t^{\mathrm{fc}}. \tag{6}$$

Consecutively, the $\mathrm{RMSE}^{\mathrm{abv}}$ follows as

$$\mathrm{RMSE}^{\mathrm{abv}} = \sqrt{\sum_{d=0}^{D-1} \frac{(E^{\mathrm{abv}}(p^{\mathrm{l}}(d)) - E^{\mathrm{abv}}(\bar{p}^{\mathrm{l}}(d))^2}{D}}. \tag{7}$$

Fig. 1. Forecasted power profiles using different algorithms.

2.3 Accuracy of Load Forecasts

For each forecasting technique, day ahead forecasts are generated for a whole year. Figure 1 shows a comparison of the different forecasts for an exemplary week in March.

In that, the profiles generated with KNN and GLM are smooth and show very few peaks or valleys. This is inherent in the methods themselves, KNN is making its predictions based the average the 40 nearest neighbors, GLM is using a Gaussian distribution as a link function in a linear regression model. In the exemplary week, MLP and the persistence algorithm show a more volatile load forecast.

To evaluate the ability to forecast peak energy we set the limit power to 95% of the yearly load peak.

This leads to the results for the whole year summarized in Table 1

In terms of the RMSE, KNN performs best followed by the linear regression, MLP, and persistence. This is similar to the results for residential households in [7]. As the RMSE penalizes outliers of forecast error an averaged forecast such as the KNN forecast performs well regarding this metric.

The ranking of the PAPE is directly opposite. Here, the persistence method has a much better PAPE than all other models. As it is a realistic load profile,

Table 1. Accuracy of load forecasts

	Pers.	MLP	GLM	KNN
RMSE/kWh	348.0	348.0	298.1	265.9
PAPE/%	74.6	229.4	254.9	595.6
RMSE^{abv}/kWh	322.8	345.2	234.5	234.5

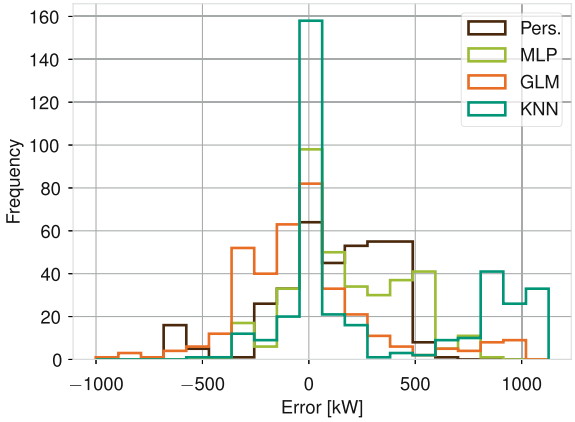

Fig. 2. Histogram of the differences between the observed peak load versus the forecasted peak load.

the persistence forecast leads to power profiles with measured peaks. Therefore, the peaks in the forecasts are close to those in measurements.

MLP and GLM have a similar ability to forecast peaks while the KNN forecast method leads to a low accuracy regarding the load peak due to the averaging. This can be explained using Fig. 2. It shows the distribution of peak load errors while positive errors resemble underestimating the actual power. Although KNN leads to the highest amount of (close to) accurate forecasts, the method underestimates the peak load many times strongly which leads to a high PAPE value. The other methods show overall smaller errors where MLP and persistence method are more likely to underestimate the load while GLM is more likely to overestimate the load profile.

The RMSE^{abv} is indicating how well the forecasting method predicts the energy that is consumed during peak loads. Having a low error rate here is important to ensure that the state of charge is high enough to support the electricity system during peak load. The GLM and KNN show the best performance here.

3 System Setup and Control

In this study we consider a small or medium enterprise with a battery system installed at the company's premises. A PV array is installed as well, generating power dependent on the solar irradiation. The remaining electric load entails a supply profile delivered by a utility through the public grid.

Our goal is to control the battery system on site for the purpose of shaping the load profile at the grid connection point. Here, the main economic driver is to reduce the peak supply power which can account for the main part of the grid usage fees.

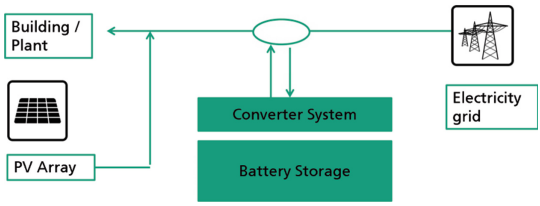

Fig. 3. Schematic overview of the studied system.

In the following, we present a simulation model of such a system. We use this model to investigate the behavior of the developed controller and evaluate its performance compared to other approaches.

3.1 Simulation Modeling of the System

To evaluate different control strategies we perform a simulation of the commercial BESS. The used simulation model is shown schematically in Fig. 3.

We assume that power profiles are measured with a constant measurement time step Δt. A profile time series consist of N time steps numbered with the time index $k = 0, \ldots, N$.

For simulation and control purposes, we denote the uncontrollable power of the electric load and the PV generation with p_k^{l} and p_k^{pv} respectively. Here, we use the index k to denote the k-th measurement at time $t_k = t_0 + k\Delta t$ with t_0 the initial time of the simulation horizon.

We summarize the uncontrollables in the residual load

$$p_k^{\mathrm{r}} = p_k^{\mathrm{l}} - p_k^{\mathrm{pv}} \tag{8}$$

As both electric load and generation are strictly positive, the residual load is positive when the load exceeds the PV generation on site. Vice versa, a negative residual load indicates that the PV generation is larger than the electric load.

The variable p_k^{b} denotes the battery power with the sign convention

$$\begin{aligned} p_k^{\mathrm{b}} \leq 0 &: && \text{discharging} \\ p_k^{\mathrm{b}} > 0 &: && \text{charging.} \end{aligned}$$

We consider systems that are connected to the AC electricity system on the site. Therefore, p_k^{b} denotes the AC power of the battery. We define the controllable variable as the AC converter power u_k.

Standby losses l^{sb} as well as power dependent conversion losses l_k^{c} apply. This leads to expressing the relation between AC and DC battery power (denoted with p_k^{dc}) as

$$p^{\mathrm{b}}(u_k) = l_k^{\mathrm{sb}} + \underbrace{l_k^{\mathrm{c}} + p_k^{\mathrm{dc}}}_{u_k}. \tag{9}$$

While the standby losses are constant, the converter losses l_k^{c} depend quadratically on the converted power

$$l_k^{\mathrm{c}}(u_k) = \begin{cases} 0 & \text{if } u_k = 0 \\ p_a + u_a u_k + r_a u_k^2 & \text{else.} \end{cases} \tag{10}$$

We model the state of the system as the state of charge of the battery denoted by x_k. Battery operation changes the state of charge from time step k to $k+1$

$$x_{k+1} = x_k + \frac{\Delta t}{C^{\mathrm{bat}}} \begin{cases} p_k^{\mathrm{dc}} \left(1 - \epsilon^{\mathrm{eff}}\right) & \text{if } p_k^{\mathrm{dc}} > 0 \\ p_k^{\mathrm{dc}} \left(1 + \epsilon^{\mathrm{eff}}\right) & \text{if } p_k^{\mathrm{dc}} < 0 \end{cases} \tag{11}$$

with a constant static battery loss ϵ^{eff}. Here, C^{bat} denotes the battery capacity and p_k^{dc} is obtained using Equations (9) and (10).

3.2 Modeling of Grid Connection

From the definitions in the previous section we obtain the power profile at the grid connection point

$$p_k^{\mathrm{g}} = p_k^{\mathrm{r}} + p_k^{\mathrm{b}}. \tag{12}$$

In accordance with the above sign convention, a positive value of p^{g} denotes grid supply. Economic costs of operation stem from this power profile.

In this study, we consider two main economic factors describing the attractiveness of a use case.

- **Reduction of the Load Peak**: Electricity customers consuming more than 100 MWh per year pay grid usage fees based on the peak electric power in each year. The peak power is obtained by the maximum of the 15 min average of the grid power profile. The distribution grid operator (DSO) assigns the resulting costs with a price per kW which vary between different DSOs.
  In the following, the peak power is denoted by

  $$p^{\mathrm{peak}} = \max(\hat{p}_0^{\mathrm{g}}, \ldots, \hat{p}_{M-1}^{\mathrm{g}}) \tag{13}$$

  where M denotes the horizon of the 15 min averages $\bar{p}_m^{\mathrm{g}}$ of the minute resolution measurement p_k^{l}.
- **Degree of Self-Sufficiency** As it is economically attractive, many commercial and industrial customers install PV generators. Although there is a remuneration for feeding PV power into the public grid, it is much lower than the consumer electricity price. Hence, the main financial benefit stems from supplying power to the plant directly as well as using the battery system as an intermediate storage.
  The ratio of energy provided by the PV generator on site in the energy consumed overall is denoted by the degree of self-sufficiency

  $$\Sigma^{\mathrm{self}} = \frac{E^{\mathrm{pv}\to\mathrm{load}}}{E^{\mathrm{load}}}. \tag{14}$$

For each individual factor, a simple control strategy is sufficient to assert optimal satisfaction of the individual objective. However, the different strategies conflict when stacking the use cases.

3.3 Control Concept and Standard Implementation

Using a perfect forecast of consumption and generation, optimization models have proven successful in weighing the different objectives discussed in the previous section [3,5]. Under a realistic, i.e., uncertain, forecast, the control strategy is less straightforward. In this early work in progress, we develop a heuristic control strategy with the goal to weigh both use cases in a realistic setup.

For the simulation study, we assume that the battery power can be controlled continuously in an interval

$$u_k \in [-p^{\text{dch, max}}, p^{\text{ch, max}}]. \tag{15}$$

Here $p^{\text{dch, max}}$ and $p^{\text{ch, max}}$ denote the maximum discharge and charge power respectively.

The battery state of charge may prohibit certain battery operation e.g., discharging of an already empty battery storage. Then, an internal controller asserts a feasible power, in this case no battery operation.

The control strategy corresponding to the pure self-sufficiency use case is equivalent to charging PV generation exceeding the load to the battery and discharging the battery to supply the load exceeding generation. It can be formalized as

$$u^{\text{ss}}(\overset{*}{p}{}^{\text{r}}_k) = -\overset{*}{p}{}^{\text{r}}_k \tag{16}$$

where the asterisk in $\overset{*}{p}{}^{\text{r}}_k$ denotes the current measurement of the residual generation.

A similar strategy exists exclusively addressing the peak shaving use case this was presented e.g. in [9]. At the beginning of the year, the plant operator determines a limit power p^{lim} from a load profile analysis in the previous year. This limit power acts as a target peak load not to be exceeded during operation. Furthermore, a threshold power $p^{\text{th}} < p^{\text{lim}}$ defines the power below which the battery is recharged from the grid.

With these two values the pure peak shaving strategy reads

$$u^{\text{ps}} = \begin{cases} -(p^{\text{r}} - p^{\text{lim}}) & \text{if } p^{\text{r}} > p^{\text{lim}} \\ 0 & \text{if } p^{\text{lim}} > p^{\text{r}} > p^{\text{th}} \\ p^{\text{th}} - p^{\text{r}} & \text{if } p^{\text{th}} > p^{\text{r}} \end{cases} \tag{17}$$

This strategy entails that the battery idles at maximum state of charge even when no peak of electric load is occurring. Then, excessive PV power can not be stored, other use cases as FCR and energy trading can also not be addressed.

Our goal is to develop a control strategy that is still able to shave peaks of the electric load while providing battery capacity for other use cases when no peaks can be expected.

This control strategy uses the forecast of the residual generation

$$\bar{p}^{\text{r}}(t_k) = \bar{p}^{\text{r}}_0, \ldots \bar{p}^{\text{r}}_{F-1} \tag{18}$$

with a forecast horizon $F = 8 \cdot 4$. Typically, the time step of the forecast is larger than the resolution of simulation data. Here, we use a time step $\Delta t^{\text{fc}} = 15\,\text{min}$

for forecasts obtained using the methods presented in Sect. 2.1. This leads to a predictive horizon of 8 h.

From the forecast an expected energy above the limit power is determined as in (6)

$$E^{\mathrm{abv}} = \sum_{f=0}^{F-1} \max(0, \bar{p}_f^{\mathrm{r}} - p^{\mathrm{lim}}) \Delta t^{\mathrm{fc}}. \tag{19}$$

With this, the multi-use control scheme is selected out of the two pure strategies.

$$u^{\mathrm{mu}} = \begin{cases} u^{\mathrm{ps}} & \text{if } E^{\mathrm{abv}} > 0 \\ u^{\mathrm{ss}} & \text{if } E^{\mathrm{abv}} = 0 \end{cases} \tag{20}$$

4 Simulation Results

We perform a simulation study showcasing the features of the developed system. Our framework is based on simulation data with a resolution of 1 min. The data stem from measuring the electric load of a medium-sized industrial plant in the area of Freiburg, Germany in 2021.

The electric load profile of an average week together with the 75% and 25% quantile of the load is shown in Fig. 4.

Overall, the measurement had minor gaps making up for 0.3 % of the time. For both the simulation and forecast generation, these gaps were filled using the last measurement prior to each gap. All gaps were shorter than 15 min except for two gaps. These gaps occurred in the night and on a weekend respectively where the load showed an approximately constant power profile before and after the gap.

The plant had a small PV generator installed. We scaled the measured production time series to a peak power of 1 MW and added a simulated battery with 600 kWh usable capacity.

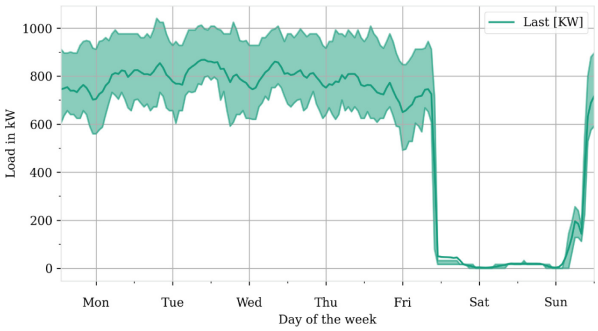

Fig. 4. Average weekly load profile of the simulation data for a medium-sized industrial plant in Freiburg, Germany.

4.1 Compared Controllers

To control the storage charging and discharging, we used the strategies described in the previous section. The used controllers are abbreviated as follows

- **Pure Peak Shaving (PS)**: Uses the control strategy from Equation (17) This controller is most likely to buffer all occurring peaks. However, the battery is charged from the grid, and hence PV power exceeding local consumption is fed into the grid.
- **Self-Sufficiency (SS)**: Controller maximizes self-sufficiency using Equation (16).
- **Multi-Use (MU)**: The proposed controller described in Equation (20). We feed the multi-use controller with different forecasts as presented in Sect. 2.1. Additionally, we simulate the behavior with the perfect forecast.

4.2 Evaluation of Operation

The goal of the controller is to shave load peaks using realistic load forecasts while simultaneously providing capacity to other use cases. Here we consider PV self-sufficiency as an exemplary second use case.

Economically, the absolute load peak as in Equation (13) causes the main cost contribution in most cases. However, this metric is linked to singular events. Hence, we calculate additional indicators

- Energy above the intended limit power
- Self-Sufficiency as defined in (14)
- Energy fed to the grid $E^{\mathrm{pv}\rightarrow\mathrm{g}}$
- Idle time while the battery is full T^{full}

4.3 Simulation Results

We perform a simulation for each controller setup. Table 2 summarizes the results in terms of the above metrics.

The two pure controllers (SS and PS) perform best in the respective category. I.e., the self-sufficiency approach reaches the highest value for the self-sufficiency Σ^{self} and the lowest grid feed-in. Similarly, the pure peak shaving strategy led to the lowest overall peak grid power.

The multi-use strategy using perfect foresight leads to both the lowest peak and highest self-sufficiency. This shows, that the algorithm is applicable in general and the chosen horizon of 8 h is sufficient to prepare for load peaks.

Using the realistic forecast does not lead to shaving the highest load peak in the year at the current state of the forecast methods with any approach. However, all forecast methods increase the self-sufficiency. Furthermore, using the MLP or the persistence approach reduced the energy consumed above a peak power. Both methods performed fairly well in forecasting the peak load.

The multi-use approach reduced the idling time at full battery state of charge significantly independent of the chosen forecast. This increases the lifetime of the battery storage.

Table 2. Results of simulation study

Method	$E^{\mathrm{pv}\to\mathrm{g}}$ MWh	Σ^{self} %	T^{full} h	E^{abv} kWh	p^{max} kW
PS	342.4	15.3	8511.2	0.0	1135.6
SS	270.4	16.7	646.4	6794.0	1265.4
MU Pers	272.2	16.6	1121.8	6618.3	1265.4
MU MLP	272.7	16.6	1240.3	4994.3	1265.4
MU KNN	270.4	16.7	646.4	6794.0	1265.4
MU GLM	270.4	16.7	646.4	6794.0	1265.4
MU Perf	271.4	16.6	870.1	131.8	1135.6

5 Conclusion and Upcoming Research Steps

In this contribution we have presented different forecast methods for load profiles and evaluated their accuracy when forecasting load peaks. Then, we used these forecasts to control a battery storage with the goal to shave the load peaks. At the current state of the control and forecast algorithms self-sufficiency can be improved compared to a pure peak shaving strategy. However, only perfect foresight leads to a reduced highest peak at the moment.

In future work, we plan to improve our algorithms for both forecast and resulting control in the following ways.

- For the current study, there was no reliable sizing method (similar to e.g., [11] for the residential case) available. A larger PV generator may increase the self-sufficiency and automatically reduce load peaks occurring during the day.
- The forecast methods will be optimized on peak accuracy. Especially forecast methods using neuronal networks (MLP in this case) offer the possibility to using a custom loss function in training. We intend to use this to include a measurement of peak accuracy in the loss function.
- Additionally, past forecast errors may be used to generate a probabilistic forecast. Then, a control algorithm can use such a forecast to increase the sensitivity on possible peaks.

Overall, the first implementation presented here indicated potential to combine different use cases using load forecasts. In contrast to optimization based algorithms, the heuristics can be implemented easily into existing battery management software such as OpenEMS. This increases the likeliness to be implemented in commercial hardware.

References

1. Kadir Amasyali and Nora M El-Gohary. A review of data-driven building energy consumption prediction studies. Renewable and Sustainable Energy Reviews, 81:1192–1205, 2018.
2. bnNetze. Hochlastzeitfenster für das Jahr 2021 in der Mittelspannung, 2020.
3. Fritz Braeuer, Julian Rominger, Russell McKenna, and Wolf Fichtner. Battery storage systems: An economic model-based analysis of parallel revenue streams and general implications for industry. Applied Energy, 239:1424–1440, April 2019.
4. Shuang Dai, Fanlin Meng, Hongsheng Dai, Qian Wang, and Xizhong Chen. Electrical peak demand forecasting- A review, August 2021.
5. Stefan Englberger, Andreas Jossen, and Holger Hesse. Unlocking the Potential of Battery Storage with the Dynamic Stacking of Multiple Applications. Cell Reports Physical Science, 1(11):100238, November 2020.
6. Jan Figgener, Peter Stenzel, Kai-Philipp Kairies, Jochen Linßen, David Haberschusz, Oliver Wessels, Georg Angenendt, Martin Robinius, Detlef Stolten, and Dirk Uwe Sauer. The development of stationary battery storage systems in Germany – A market review. Journal of Energy Storage, 29:101153, June 2020.
7. Arne Groß, Antonia Lenders, Friedhelm Schwenker, Daniel A. Braun, and David Fischer. Comparison of short-term electrical load forecasting methods for different building types. Energy Informatics, 4(3):13, September 2021.
8. Rob J. Hyndman and George Athanasopoulos. Forecasting: Principles and Practice. OTexts, Melbourne, Australia, second edition, 2018.
9. Christopher Lange. Energiesektoren-übergreifende Lastspitzenreduktion mit elektrischen und thermischen Energiespeichern. PhD thesis, Friedrich-Alexander-Universität Erlangen-Nürnberg (FAU), 2021.
10. D. W. van der Meer, J. Widén, and J. Munkhammar. Review on probabilistic forecasting of photovoltaic power production and electricity consumption. Renewable and Sustainable Energy Reviews, 81:1484–1512, January 2018.
11. Johannes Weniger, Tjarko Tjaden, and Volker Quaschning. Sizing of residential PV battery systems. In 8th International Renewable Energy Storage Conference and Exhibition, 2013.
12. Baran Yildiz, Jose I Bilbao, and Alistair B Sproul. A review and analysis of regression and machine learning models on commercial building electricity load forecasting. Renewable and Sustainable Energy Reviews, 73:1104–1122, 2017.